

## Picosecond transient photoconductivity in poly(*p*-phenylenevinylene)

C. H. Lee, G. Yu, D. Moses, and A. J. Heeger

*Institute for Polymers and Organic Solids and Department of Physics, University of California at Santa Barbara, Santa Barbara, California 93106*

(Received 25 March 1993)

We report the results of transient-photoconductivity measurements on films of poly(*p*-phenylenevinylene) (PPV) in the subnanosecond-time regime. The initial fast transient photocurrent decays exponentially with a decay time of about 100 ps, followed by a slower component with a decay time of about 600 ps. The magnitude of the fast component is proportional to the light intensity and independent of temperature, while the magnitude of the slower component is proportional to the square root of the light intensity and decreases as temperature decreases with a thermal-activation energy of about 100 meV. We attribute the initial response to photogenerated electrons and holes (polarons) and the following slower decay to bipolarons in the nondegenerate ground-state conducting polymer. Measurements of the spectral response of both transient and steady-state photoconductivity demonstrate that the onset of the photoconductivity coincides with that of photoabsorption, consistent with the photogeneration of free carriers via an interband transition. The interpretation of the initial temperature-independent transient photocurrent as the displacement current from the field-induced polarization of neutral excitons is ruled out by careful analysis of the transient-photocurrent data and by direct measurements on polydiacetylene-(toluene sulfonate), a conjugated polymer with a known exciton binding energy ( $E_{exc}$ ),  $E_{exc} \approx 0.4$  eV. A variety of measurements has enabled us to set an upper limit on  $E_{exc}$  in PPV and several of its alkoxy derivatives;  $E_{exc}$  is comparable to, or less than,  $k_B T$  at room temperature.

### I. INTRODUCTION

Photoexcitation of nondegenerate ground-state conducting polymers provides a method for photogenerating polarons ( $P^\pm$ ) and bipolarons ( $B^{2\pm}$ );<sup>1</sup> these charged excitations can be studied through measurements of photoconductivity (PC), excitation spectroscopy, and photoluminescence (PL). Such studies have taken on special significance following the demonstration that poly(*p*-phenylenevinylene) (PPV) and its derivatives can be used as the active luminescent layer in electroluminescent light-emitting diode devices.<sup>2-5</sup>

The electronic structure of conjugated macromolecular chains (conducting polymers) has been described in terms of a quasi-one-dimensional tight-binding model in which the  $\pi$  electrons are coupled to distortions in the polymer backbone by the electron-phonon interaction.<sup>1</sup> In this model, photoexcitation across the  $\pi$ - $\pi^*$  band gap creates free carriers (electrons and holes) as in conventional semiconductors. Chain relaxation causes the photogenerated free carriers to become localized and form the nonlinear excitations of conducting polymers: solitons, polarons, or confined soliton pairs (bipolarons), depending on the ground-state degeneracy.

In systems with degenerate ground state, or in systems where the confinement is relatively weak, spinless solitons are the important charged excitations. Direct photoexcitation of soliton-antisoliton pairs (at energies well below that of the interband transition) is enabled by the Franck-Condon overlap between the uniform chain in the ground state and the distorted chain in the excited state.<sup>6</sup>

In nondegenerate ground-state conducting polymers,

photoexcitation creates electron-hole pairs which separate as free charge carriers (and contribute to PC) and/or recombine to form neutral polaron excitons (or neutral bipolarons). The *direct* photogeneration of polarons (electrons and holes "dressed" with a local chain relaxation) is also enabled by the Franck-Condon overlap between the uniform chain in the ground state and the distorted chain in the excited state.<sup>7</sup> When relaxation in the excited state (to form polarons) is important, the photoabsorption exhibits characteristic vibronic sidebands.<sup>7</sup>

The neutral polaron-exciton channel results from the combined effects of the screened Coulomb attraction between opposite charge carriers and the lattice confinement which lowers the total energy when two polaron distortions overlap.<sup>8</sup> Polaron excitons can decay radiatively, detected as PL, or nonradiatively. Both intrachain and interchain photogeneration of the charge carriers are possible; in either case, however, the radiative recombination is predominantly intrachain as demonstrated by the anisotropic PL in highly oriented materials.<sup>7,9</sup>

A variety of experimental studies have clearly established that polarons and bipolarons are formed in PPV after photoexcitation.<sup>10</sup> In addition to the charged photoexcitations, triplet polaron excitons have been identified by photoinduced absorption<sup>11,12</sup> (PA) and absorption-detected magnetic resonance.<sup>13</sup>

The mechanism for photogeneration of charge carriers is not fully understood. It is not clear at present whether the photoconductive response of PPV results principally from secondary processes following the photogeneration of neutral geminate pairs (i.e., bound Wannier-type excitons) as would be the case if electron-electron interactions

were of major importance,<sup>14,15</sup> or from separated free positive and negative charge carriers as would be the case if the screened electron-electron interactions were relatively weak compared to the electron-phonon interaction.<sup>16</sup> Subnanosecond transient PC experiments offer the possibility of monitoring the generation, transport, and recombination of charge carriers before their transport is limited by traps.<sup>17-22</sup> In addition, when compared with data from time-resolved PA and PL, transient photoconductivity provides insight into the carrier photogeneration and recombination processes.

The transient PA measurements are not yet available for PPV, but they have been reported for its alkoxy derivative.<sup>23</sup> Transient PL experiments have been reported for PPV (Refs. 9 and 24(a)) and for the branched alkoxy derivative of PPV.<sup>24(b)</sup> Prior to this work, transient PC data for PPV have been limited to nanosecond time resolution.<sup>16</sup> Thus the initial fast photoconductive response of charge carriers has not been resolved in sufficient detail to enable the comparisons with PA and PL. The PC response at early times is especially important for understanding the photogeneration mechanism of charged carriers because the delayed slower component and the steady state response are dominated by trap-limited transport.<sup>17-22</sup>

The results of PA (Refs. 10 and 11) measurements on PPV imply that the long-lived charge carriers are bipolarons: the infrared active vibrational modes and the characteristic pair of subgap electronic absorption bands are the signatures of bipolarons.<sup>25</sup> However, bipolarons cannot be directly photogenerated; they are formed through  $P^{\pm} + P^{\pm} \rightarrow B^{2\pm}$ , and then contribute to the photoconductivity.<sup>26</sup> Moreover, spin-dependent photomodulation experiments<sup>13</sup> showed that the long-lived charged excitations are associated with spinless features in PA whose recombination (or generation) is spin dependent, consistent with the bipolaron generation through  $P^{\pm} + P^{\pm} \rightarrow B^{2\pm}$ . Since polarons can be *directly* photogenerated<sup>7,8</sup> and since simulations show that chain distortions form around an electron or a hole in times less than  $10^{-13}$  s,<sup>27</sup> transient PC is likely to be dominated by polaron transport in the picosecond time regime and by bipolarons at later times.<sup>20</sup>

We present the results of a series of measurements of the transient PC (in the subnanosecond-time domain) of PPV including the temperature dependence, light intensity dependence, electric-field dependence, and the spectral response. The picosecond transient PC reveals a fast initial response which decays exponentially with time constant of about 100 ps, followed by a slower component with a decay time of about 600 ps. The magnitude of the fast component is proportional to the light intensity and independent of temperature, while the magnitude of the slower component is proportional to the square root of the light intensity and decreases as temperature decreases with an activation energy of about 100 meV.

The displacement current contribution to the fast transient photocurrent is carefully and quantitatively considered. The experimental results are not consistent with the displacement current contribution which would arise from the electric-field-induced polarization of

bound excitons. Moreover, direct measurements on polydiacetylene-(toluene sulfonate), a conjugated polymer with a known exciton binding energy ( $E_{exc}$ ),  $E_{exc} \approx 0.4$  eV, demonstrate that this displacement current contribution would be more than two orders of magnitude weaker than the initial transient response in PPV.

We recently reported that the onset of the steady-state PC of PPV coincides with the onset of photoabsorption and that the PC spectrum can be quantitatively understood within the semiconductor energy band picture.<sup>26</sup> We find that the onset of the picosecond transient PC also coincides with that of absorption and the steady-state PC, in further support of this conclusion. Moreover, the relatively large, temperature-independent initial (i.e.,  $t \rightarrow 0$ ) photoconductivity independently implies the photogeneration of *free* carriers (rather than bound excitons) via an interband transition. We therefore attribute the initial photoconductive response to photogeneration of free charge carriers via the interband ( $\pi$ - $\pi^*$ ) transition in the context of the semiconductor energy-band model of the electronic structure. The following slower decay arises from transport via bipolarons (polaron pairs confined by the electron-phonon interaction in the nondegenerate ground-state conducting polymer).

The conclusion that in PPV the photoexcitations are free carriers (as in a band model), rather than bound excitons, is supported by a variety of experimental results which we briefly summarize.

## II. EXPERIMENT

Samples used for this study were thin films of PPV prepared via the precursor route. The water-soluble precursor<sup>28</sup> polymer was first spin cast onto  $\frac{1}{2}$ -square-in. glass or alumina substrates (spin speed 800–1000 rpm) under nitrogen gas. The precursor film was then sealed in an evacuated tube and converted into the conjugated form by heat treatment at 300°C for 3 h. Sample thicknesses were in the range of about 0.2–0.3  $\mu\text{m}$ , with corresponding optical densities of about 2.5 at the peak in the absorption spectra. The steady-state PC was measured using the standard lock-in technique; transmission spectra were obtained with a Perkin-Elmer Lambda-9 spectrophotometer. Details of the sample preparation and the steady-state PC measurement have been reported previously.<sup>26</sup>

For the subnanosecond transient PC measurement, the Auston switch transmission line configuration<sup>29</sup> was used; gold stripline electrodes were evaporated onto the converted PPV film on an alumina substrate and a gold backplane was evaporated onto the back surface of the alumina substrate (area 0.5 in.  $\times$  0.5 in. and thickness 0.65 mm) to form a transmission line with 50- $\Omega$  impedance and with a frequency response over 100 GHz. The electrodes were 0.6-mm wide and the gap between electrodes was 0.1 mm. Details about the Auston switch configuration can be found in our early publications.<sup>17-20</sup> The dark conductivity of the PPV films is estimated to be about  $5 \times 10^{-9}$  S/cm at room temperature with an activation energy of about 210 meV, as measured with a Keithley 467 picoammeter/voltage source.<sup>26</sup> The dark I-V mea-

surement shows Ohmic behavior up to at least 200-V bias voltage across the 0.1-mm gap (electric field of  $2 \times 10^4$  V/cm).

Excitation pulses were obtained from a PRA (Photochemical Research Assoc., Inc.) LN105 dye laser pumped with a PRA LN1000  $N_2$  laser, operated at a repetition rate of 3–5 Hz. The pulse width was approximately 20–30 ps and the typical light intensity was about  $2 \mu\text{J}/\text{pulse}$ , corresponding to the incident photon flux of about  $3 \times 10^{15}$  photons/cm<sup>2</sup>. Photon energies were varied (by changing the dye) from 1.9 to 2.9 eV.

One side of the microstrip was biased with a dc voltage and the other side was connected to a EG&G PAR (Princeton Applied Research) 4400 boxcar system fitted with a Tektronix S-4 sampling head. The boxcar was triggered with the light pulse via a photodiode. The temporal resolution of the electronic detection system was about 50 ps (as measured by the rise time of the photocurrent), resulting from a combination of the gatewidth and trigger jitter of the boxcar (EG&G PAR 4400 system with a Tektronix S-4 sampling head) and the response of the cable transmission line between the probe and the boxcar.

Data were obtained with uniform illumination of the sample across the 0.1-mm gap. The photon energy was at  $\hbar\omega = 2.92$  eV (425 nm) and the biasing electric field was  $2 \times 10^4$  V/cm, unless otherwise specified. Samples were mounted onto the cold finger of a Helitran cryostat, and the measurements were carried out under a vacuum of less than  $10^{-4}$  Torr. Experiments were carried out in the temperature ranges from 360 to 81 K. To improve the signal-to-noise ratio, signal averaging was employed, and the data were base line corrected to the dark response. For measurements of the light-intensity, electric-field, and temperature dependences of the transient PC, the photocurrent was amplified by a 1.1-GHz-bandwidth amplifier, and the signals from 100 laser pulses were averaged. Light intensity was changed by using neutral density filters. During the measurement, we monitored the light intensity by splitting part of pulse light (using a beam splitter) into the photodiode connected to the Tektronix 468 digital storage oscilloscope.

### III. RESULTS OF THE TRANSIENT-PHOTOCONDUCTIVITY MEASUREMENTS

Figure 1(a) shows the time-resolved transient photocurrent of a PPV film biased with an electric field of  $2 \times 10^4$  V/cm; data are shown for the sample at room temperature and at 81 K. The excitation laser pulses were at  $\hbar\omega = 2.92$  eV (425 nm) with a 20-ps pulse width. The photon flux incident onto the sample per pulse was about  $3 \times 10^{15}$  photons/cm<sup>2</sup> ( $\approx 2 \mu\text{J}$  per pulse). The same PC data are shown on a semilog plot in Fig. 1(b). The data in Fig. 1 are the results of a 20-sweep average to improve the signal-to-noise ratio. The solid curves assume the following form:

$$I_{\text{ph}}(t) = A_1 \exp(-t/\tau_1) + A_2 \exp(-t/\tau_2). \quad (1)$$

Because the slower component is suppressed at lower temperature, the initial fast decaying component is more clearly resolved at 81 K.

The photoresponse turns on extremely fast as observed

previously in *trans*-(CH)<sub>x</sub> (Refs. 17 and 21) and P3HT;<sup>20</sup> the rise time and the initial decay of the asymmetric peak results from a convolution of the pulse width of the pump beam and rise times of the electronic detection system; we are not able to resolve the initial time response of the photocurrent. The decay of the picosecond PC fits quite well to the sum of two exponentials, Eq. (1); for the initial fast decay  $\tau_1 \approx 100$  ps while for the slower exponential decay  $\tau_2 \approx 600$  ps. Recently, the initial fast decay in *trans*-(CH)<sub>x</sub> was shown to be approximately 7 ps using the photoconductivity cross-correlation technique.<sup>22</sup> In PPV the intrinsic initial decay time is probably also much less than 100 ps. Earlier work on *trans*-(CH)<sub>x</sub> (Refs. 17 and 21) and on PPV derivatives<sup>30</sup> reported that the transient photocurrent can also be fit to the two exponential decay of Eq. (1).

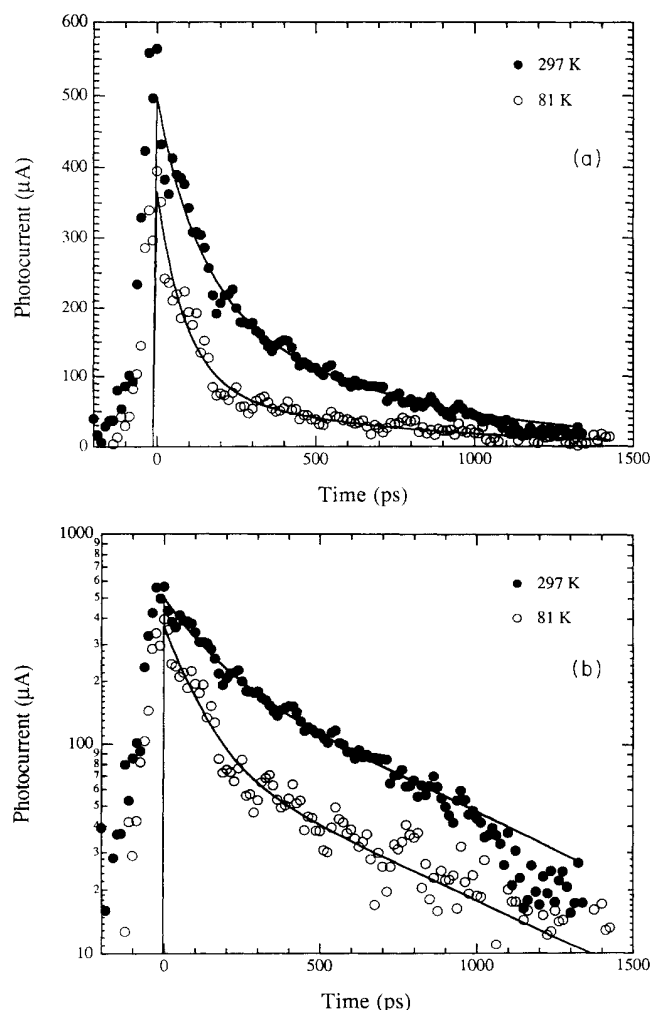


FIG. 1. (a) Time-resolved transient photocurrent of a PPV film biased with an electric field of  $2 \times 10^4$  V/cm; data are shown for the sample at room temperature (solid circles) and at 81 K (open circles). The photon flux incident onto the sample per pulse was about  $3 \times 10^{15}$  photons/cm<sup>2</sup> at 2.92 eV. The solid curves are the fits assuming the two exponential form of decay. (b) The same PC data in (a) on a semilog plot; the initial fast decay component is more clearly resolved at 81 K because the slower component is suppressed at lower temperature.

By analyzing the PC decay curves obtained from PPV at room temperature and at 81 K, we found that the magnitude of the fast component is independent of temperature, whereas that of the slower component decreases with decreasing temperature; the fitting parameters are summarized in Table I. The temperature dependence of the peak transient photocurrent from 360 to 81 K is shown in Fig. 2; the magnitudes of the fast and slower components at 297 and 81 K are indicated. Figure 2 clearly shows that the temperature dependence of the peak photocurrent is due to that of the slower component. For the measurement of the temperature dependence, the incident photon flux was about  $1 \times 10^{15}$  photons/cm<sup>2</sup> at 2.92 eV under a biasing electric field of  $2 \times 10^4$  V/cm. The beam size was increased to cover the gap completely to reduce any error arising from slight changes in beam position resulting from thermal expansion of sample holder. The photocurrent was amplified with a 1.1-GHz-bandwidth amplifier and averaged over 100 laser pulses. To assure constant light intensity at each temperature, we monitored the light intensity with the photodiode connected to the digital oscilloscope.

We estimate a lower limit for the initial photoconductivity (at the peak of the initial response) to be about 0.05 S/cm from the peak transient photocurrent in Fig. 1;  $I_{ph}(\max) \approx 564 \mu\text{A}$ , corresponding to a current density of approximately  $10^3$  A/cm<sup>2</sup> under an electric field of  $2 \times 10^4$  V/cm at room temperature. A similar magnitude of the transient photoconductivity in PPV was reported by Bradley *et al.*<sup>16</sup> By estimating the number of charge carriers and absorbed photons following the procedure used in PPV (Ref. 16) and *trans*-(CH)<sub>x</sub>,<sup>21,31</sup> one obtains the carrier migration length  $l \approx 110 \text{ \AA}$  and the mobility  $\mu \approx 0.6 \text{ cm}^2/\text{Vs}$  at room temperature. These values estimated in the subnanosecond-time regime are about an order larger than those estimated in the nanosecond-time regime.<sup>16</sup> However, since the response is still limited by the instrumental resolution, these values represent only lower limits. The transient photoconductivity of PPV is comparable to that reported for *trans*-(CH)<sub>x</sub> under similar experimental conditions, in which  $\sigma_{ph} \approx 0.3 \text{ S/cm}$  corresponds to an initial mobility of approximately  $1 \text{ cm}^2/\text{Vs}$ .<sup>17</sup> An initial mobility of  $\mu > 20 \text{ cm}^2/\text{Vs}$  was reported from the recent measurement of the picosecond PC in *trans*-(CH)<sub>x</sub> with the improved time resolution.<sup>22</sup> Thus charge carriers responsible for the initial photoresponse are highly mobile for times less than 10 ps, after which they are trapped.

The transient peak photoconductivity (at an incident photon flux of  $\sim 1 \times 10^{15}$  photons/cm<sup>2</sup> at  $\hbar\omega = 2.92 \text{ eV}$ ) is six orders of magnitude larger than the steady-state photo-

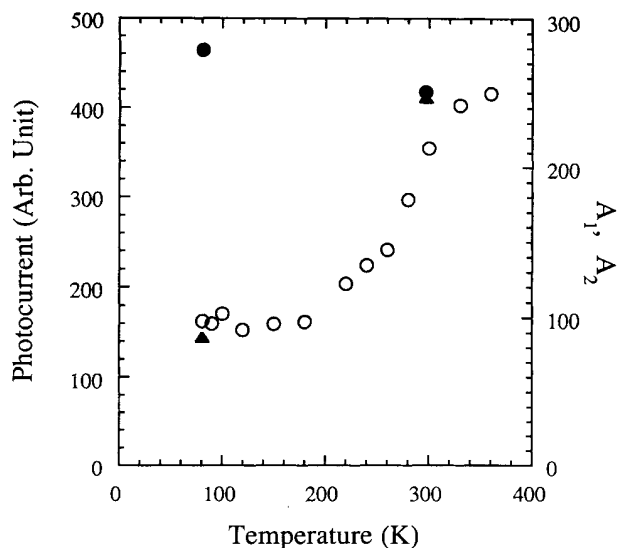


FIG. 2. Temperature dependence of the peak transient photocurrent from 360 to 81 K (open circles); the magnitudes of the fast (solid circles) and slower (solid triangles) components at 297 and 81 K are indicated.

conductivity (cw  $\sigma_{ph} \approx 6 \times 10^{-8} \text{ S/cm}$  at an incident photon flux of  $\sim 1 \times 10^{15}$  photons/cm<sup>2</sup>s at  $\hbar\omega = 2.45 \text{ eV}$ ).<sup>26</sup> The latter is also about an order of magnitude larger than the dark conductivity ( $\sigma_d \approx 5 \times 10^{-9} \text{ S/cm}$ ); these data are compared in Fig. 3 where the temperature dependences of the transient PC, the steady-state PC, and the dark conductivity are presented on a semilog plot. The transient PC shows a weak temperature dependence above about 200 K, and it is independent of temperature below 200 K (Fig. 2 demonstrates that the temperature dependence of the transient peak photocurrent is due to the slower component). The activation energy of the steady-state PC is approximately 140 meV, whereas the activation energy of the dark conductivity is about 210 meV.<sup>26</sup> The temperature range in Fig. 3 is not large enough, however, to determine whether the dependence is truly activated (note the curvature of the data on the semilog plot of Fig. 3). In conducting polymers, Mott's variable range hopping conductivity<sup>32</sup> is often used to explain the temperature dependence of the dark conductivity.<sup>33</sup>

Figure 4 shows the temperature dependence of the peak transient PC following photoexcitation with different light levels; the incident light intensity was changed from 1.6 to 0.06  $\mu\text{J}$  using appropriate neutral density filters. We found that the temperature depen-

TABLE I. Results of the two exponential fits to the curves of the transient PC decay.

$T$ (K)	$I$ (mJ/pulse)	$I_p$ (mA)	$A_1$ (mA)	$t_1$ (ps)	$A_2$ (mA)	$t_2$ (ps)
297	2	564	251	128	247	601
297	1	262	114	128	155	601
81	2	395	279	92	87	631
81	1	240	131	92	75	631

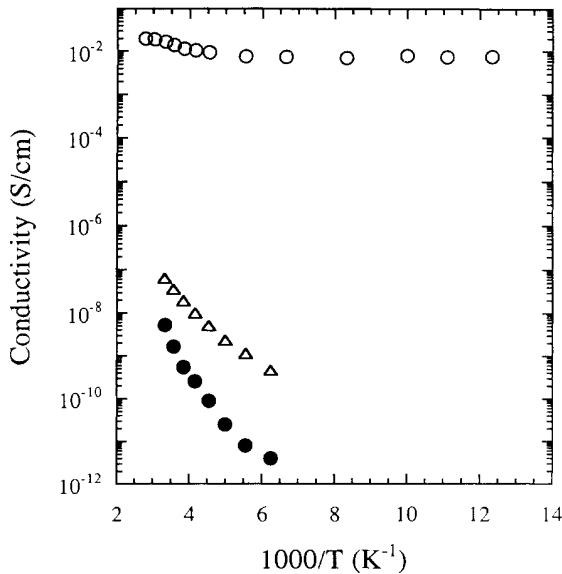


FIG. 3. Temperature dependence of the peak transient PC (open circles), steady-state PC (open triangles) and the dark conductivity (solid circles) all on a semilog plot.

dence of the transient PC above 200 K becomes even weaker as the light intensity is increased. This observation implies that the temperature-independent fast component increases faster than the activated slower component as intensity increases.

The data of Figs. 3 and 4 provide clear evidence against the bolometric contribution to the photoresponse (i.e., an increase in  $\sigma_d$  due to heating rather than a genuine photocurrent results from photoexcited carriers).

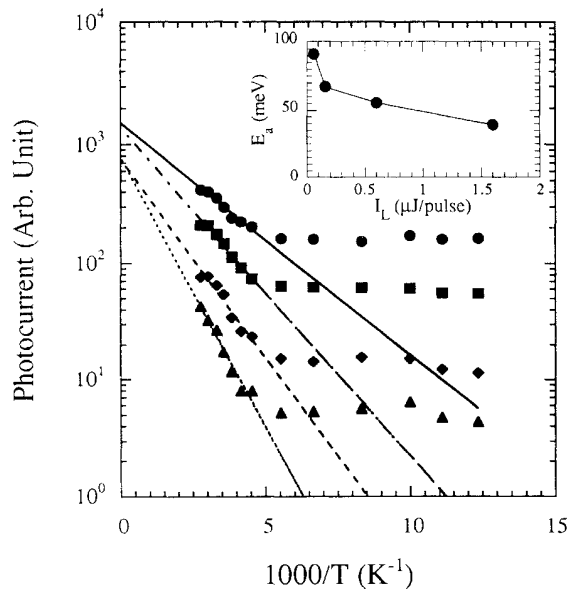


FIG. 4. Temperature dependence of the peak transient PC following photoexcitation at different levels; 1.6  $\mu\text{J}/\text{pulse}$  (circles), 0.6  $\mu\text{J}/\text{pulse}$  (squares), 0.16  $\mu\text{J}/\text{pulse}$  (diamonds), and 0.06  $\mu\text{J}/\text{pulse}$  (triangles). The inset shows the "apparent activation energies" (see text) above 200 K at different photoexcitation levels.

To obtain the activation energy of the slower component, one needs to carefully subtract the temperature-independent component from the peak photocurrent. In Fig. 5, we plot the temperature dependence of the slower component, the peak photocurrent minus the 81-K photocurrent, from 360 to 220 K in a semilog plot (the 81-K data contain only the fast component because the time-resolved data in Fig. 1 show that at 81 K the slower component is negligible compared to the fast component). From the data in Fig. 5, an activation energy  $E_a \approx 100$  meV can be estimated. This is to be comparable with  $E_a \approx 140$  eV for the steady-state PC and  $E_a \approx 210$  meV for the dark conductivity, as shown in Fig. 3. These (similar) small activation energies suggest trap-dominated transport with multiple release and retrapping of the long-lived photocarriers which contribute to the photoconductivity over the full temporal range from nanoseconds to steady state. The long-lived photocarriers thermalize into deeper traps below the mobility edge as time progresses. In this context, the temperature independence of the picosecond photocurrent implies pretrapping transport (see Sec. IV for a discussion which rules out a significant contribution from the displacement current due to field-induced polarization). Thus the rapid decay ( $\approx 100$  ps) of the temperature-independent fast component of the transient photocurrent response results from initial trapping, as in P3HT.<sup>20</sup>

Figure 6 shows the peak photocurrent (a combination of fast and slower component) at room temperature, 140 K, and 81 K as a function of the light intensity spanning a range of more than two orders of magnitude. The 140- and 81-K data show linear intensity dependences; however, at 300 K, the peak photocurrent shows a sublinear intensity dependence  $I^{0.8}$ , consistent with the data of Bradley *et al.*,<sup>16</sup> who also reported a sublinear intensity

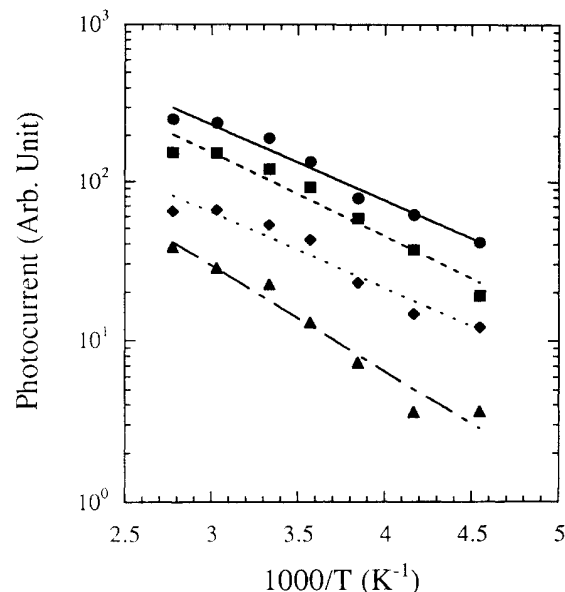


FIG. 5. Temperature dependence of the slower component of the peak transient PC, the peak PC data in Fig. 4 minus the 81 K PC data, from 360 to 220 K in a semilog plot;  $E_a \approx 100$  meV is obtained for the slower component.

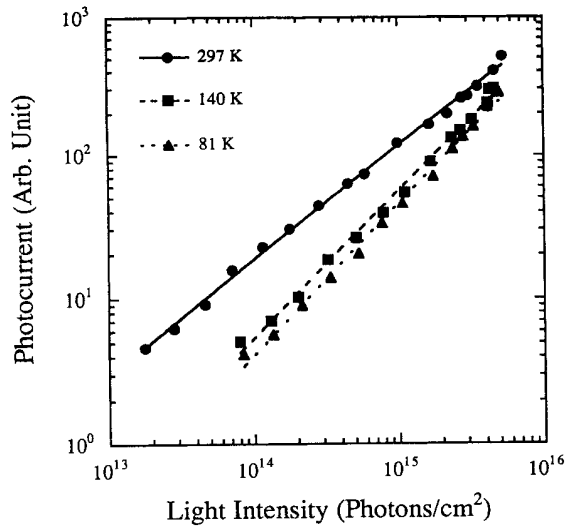


FIG. 6. Light-intensity dependence of the peak photocurrent (which consists of fast and slower component) at room temperature (circles), 140 K (squares), and 81 K (triangles).

dependence in nanosecond-time regime  $I^{0.7}$  at 300 K. This sublinear dependence is, however, an artifact; for the fast and slow components have different intensity dependences.

The intensity dependences of both the fast component (peak photocurrent at 81 K in Fig. 4) and the slower component (the latter at 360, 300, and 220 K) are shown in Fig. 7. The slower component was obtained by subtracting the 81-K photocurrent from the peak photocurrent as in Fig. 5. The intensity dependences of the two are quite different. The fast component of peak photocurrent is linearly proportional to the light intensity.

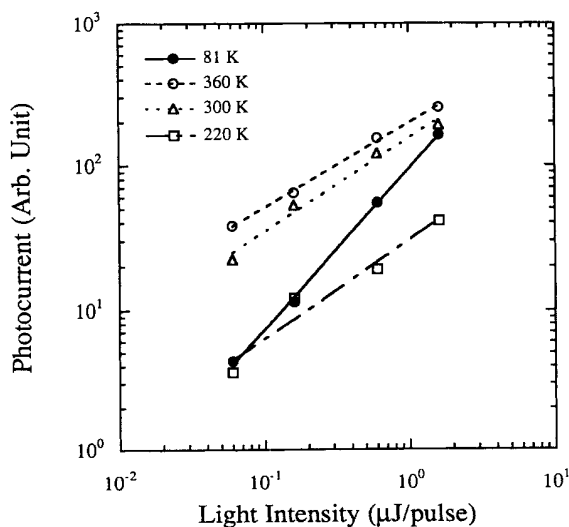


FIG. 7. Light-intensity dependence of the fast component, peak photocurrent at 81 K in Fig. 4 (solid circles), and the slower components at 360 K (open circles), 300 K (open triangles), and 220 K (open squares). The slower components were obtained by subtracting the 81 K photocurrent from the peak photocurrent as in Fig. 5.

The intensity dependence of the slower component is approximately  $I^{0.5}$ ; the slight deviations from the square-root dependence are mainly due to errors in separating the slower component from the peak photocurrent by simply subtracting the 81-K photocurrent (the data in Fig. 7 yield  $I^{0.59}$  at 360 K,  $I^{0.65}$  at 300 K, and  $I^{0.68}$  at 200 K).

A linear intensity dependence of peak photocurrent in the subnanosecond regime was previously observed in *trans*-(CH)<sub>x</sub> (Ref. 21) and P3HT.<sup>20</sup> An  $I^{0.54}$  intensity dependence was reported for the steady-state photocurrent excited at 2.82 eV by Tokito *et al.* in PPV.<sup>34</sup> The different intensity dependences of the fast and slower component explain the apparent decrease of the activation energy for higher photoexcitation levels, observed in Fig. 4, because the temperature-independent fast com-

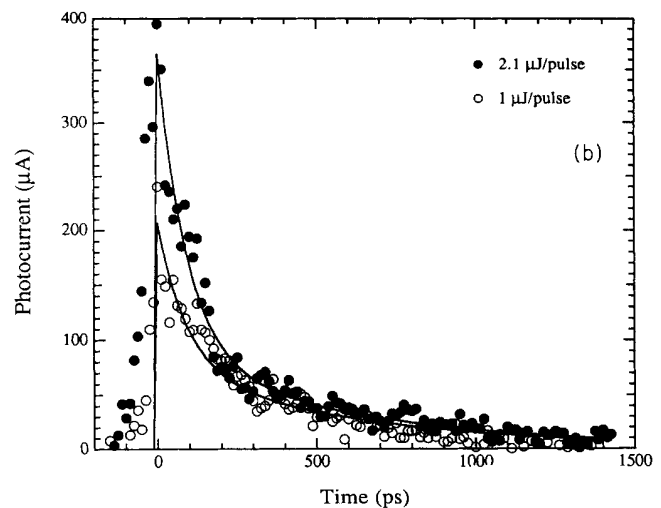
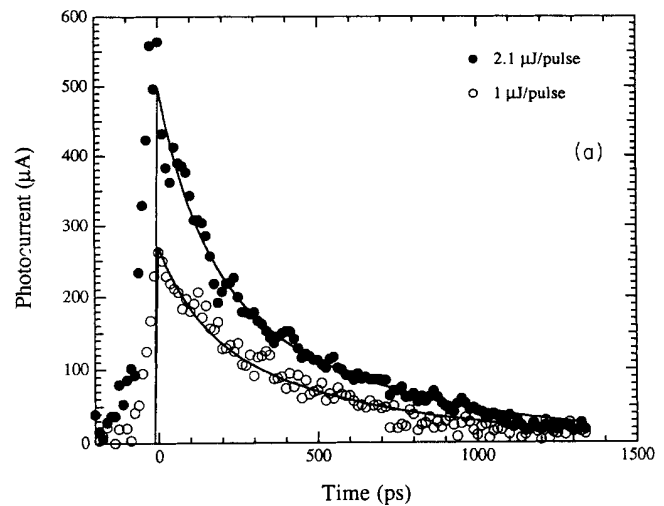


FIG. 8. Time-resolved transient photocurrent wave forms under different photoexcitation levels, 2.1  $\mu\text{J}/\text{pulse}$  (solid circles) and 1  $\mu\text{J}/\text{pulse}$  (open circles); data are shown for the sample at (a) room temperature and (b) 81 K. Wave forms were taken in the same experimental conditions as described in Fig. 1. The results of the two-exponential fit (solid lines) to the transient photocurrents are shown in Table I.

ponent contributes more to the observed peak photocurrent for higher photoexcitation levels.

The different intensity dependences of the fast and slower components are also clearly observed from time-resolved photocurrent wave forms in response to different photoexcitation levels, 2.1 and 1  $\mu\text{J}/\text{pulse}$ , as shown in Fig. 8(a) at room temperature and in Fig. 8(b) at 81 K. The wave forms were taken using the same experimental conditions as described in Fig. 1. The results of the two-exponential fit to the transient photocurrents in Fig. 8 are shown in Table I. At both temperatures, the initial peak values increase in proportion to the increase in light intensity while the increase of the slower component at later times shows the sublinear intensity dependence. The transient photocurrent wave forms in Fig. 8 demonstrate that the decay times are nearly independent of light intensity and temperature (however, the ratio of the contributions to the photocurrent from the initial and slower components does change).

Figure 9 shows the voltage dependence of peak photocurrent both at room temperature and at 81 K (incident photon flux of about  $10^{15}$  photons/cm<sup>2</sup> at 2.92 eV). At both temperatures, the peak photocurrent increases approximately in proportion to the biasing electric field. At high light levels, however, the photocurrent shows a slight sublinear voltage dependence, reminiscent of similar effects observed in P3HT (Ref. 20) and polyaniline.<sup>35</sup> The latter behavior typically arises from a combination of charging at imperfect contacts. The steady-state photocurrent and dark current also exhibit a linear voltage dependence.

The decay of the transient photocurrent seems to be independent of the photon energy for excitation at energies above the band gap. At photon energies of 2.78 eV (445 nm) and 2.58 eV (481 nm), we obtained curves identical to those shown in Figs. 1 and 8, for which the photon energy was 2.92 eV (425 nm).

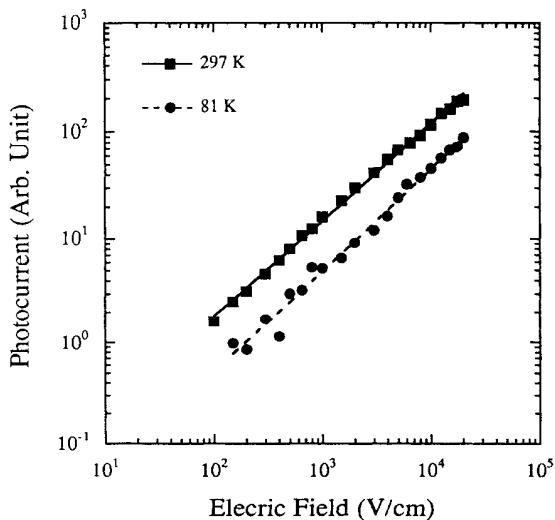


FIG. 9. Electric-field dependence of the peak transient photocurrent both at room temperature (squares) and at 81 K (circles) under the incident photon flux of about  $10^{15}$  photons/cm<sup>2</sup> at 2.92 eV.

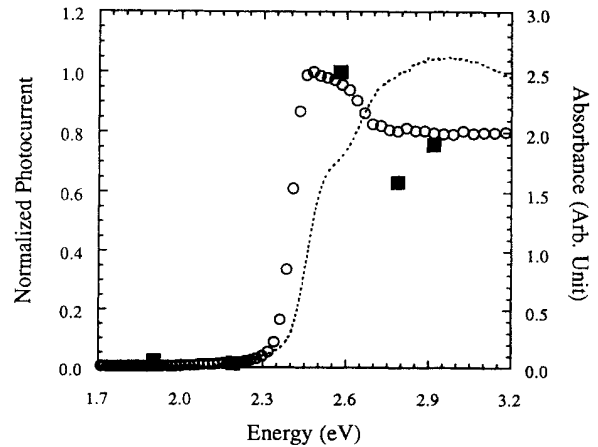


FIG. 10. Spectral response of the peak transient PC (solid squares). The steady-state PC (open circles) and optical absorption spectra (dotted line), reported in Ref. 26, are included for comparison. Both the transient PC and the steady-state PC are normalized to the equal incident photon flux and divided by their maximum PC. The transient PC at 2.92 eV is  $\sigma_{\text{ph}} \approx 0.05$  S/cm for an incident photon flux of  $\sim 3 \times 10^{15}$  photons/cm<sup>2</sup>, and the steady-state PC at 2.45 eV is  $\sim 7 \times 10^{-9}$  S/cm for an incident photon flux of  $\sim 1 \times 10^{15}$  photons/cm<sup>2</sup>s with a modulation frequency of 19 Hz.

In Fig. 10, we plot the magnitude of the peak transient PC at different photon energies. The steady-state PC and optical absorption spectra, reported in Ref. 26, are included for comparison. The transient and steady-state PC data come from samples cast from the same batch of solution. Moreover, the results of the steady-state PC experiment and the absorption experiment were taken from the same polymer film on a glass substrate.<sup>26</sup> Both the transient PC and the steady-state PC are normalized to equal incident photon flux. The measurements of the spectral response show that the onset of both the transient and the steady-state PC closely coincide with that of the optical absorption. The quantitative comparison of the onset of the steady-state PC and the optical absorption has been presented in Ref. 26, where the structure in the PC spectrum can be quantitatively predicted from DeVore's theory.<sup>36</sup> Within the limited spectral resolution available, the transient-photoconductivity response follows that of the steady-state photoconductivity.

#### IV. DISCUSSION

##### A. Does the fast transient "photoconductivity" in PPV arise from a displacement current generated by electric-field-induced polarization of bound excitons?

Recently, it was argued that the optical properties of PPV and its derivatives are not properly described within the context of band theory; a strongly correlated (Wannier) exciton model was invoked in which the exciton binding energy is large compared to  $k_B T$  (i.e., several tenths of an electron volt).<sup>14,15</sup> In the strongly correlated picture, optical absorption creates neutral excitons (electron-hole pairs bound by their Coulomb attraction

and any subsequent lattice relaxation).<sup>14</sup> The generation of charge carriers after photoexcitation is proposed to result from dissociation of excitons in the presence of the external electric field (or from exciton-exciton interaction) in the context of the Onsager model<sup>37</sup> of geminate recombination.<sup>14,15</sup>

Assuming the validity of the exciton picture, the temperature-independent transient PC would result from the displacement current generated by the electric-field-induced polarization of bound excitons. If photoexcitation creates excitons in an applied electric field  $E$ , the excitons would be polarized with the following induced electric dipole moment:

$$p = \epsilon_0 \alpha_{\text{exc}} E, \quad (2)$$

where  $\epsilon_0$  is the permittivity of free space and  $\alpha_{\text{exc}}$  is the polarizability of the exciton. Because of this photoinduced change in polarization, surface charges would build up in a time equal to the stripline response time  $2Z_0C_g \approx 2$  ps, where the characteristic impedance  $Z_0$  and the input capacitance  $C_g$  of the Auston microstripline switch are  $Z_0 = 50 \Omega$  and  $C_g = 0.02$  pF, respectively.<sup>29,38</sup>

If we assume the observed fast transient photocurrent is the displacement current, the polarizability of the exciton is given by

$$\alpha_{\text{exc}} = \frac{1}{\epsilon_0 N_{\text{exc}} E} \int_0^\infty j(t) dt, \quad (3)$$

where  $N_{\text{exc}}$  is the density of photoexcited excitons and  $j(t)$  is the photocurrent density.

By integrating the fast transient PC in Fig. 1(a), we would estimate the polarizability of the exciton [from Eq. (3)] to be  $\alpha_{\text{exc}} \approx 10^6 \text{ \AA}^3$ . This estimated polarizability is a lower bound; the density of photoexcited excitons was assumed to be equal to the density of photons absorbed, while in reality, recombination is occurring during the time of the initial transient photocurrent pulse (i.e., during the first 100 ps).

This large value of the polarizability can be used to set an upper limit on the exciton binding energy. This value for  $\alpha_{\text{exc}}$  is more than two orders of magnitude larger than the exciton polarizability in polydiacetylene-[1,6-di(*n*-carbazolyl)-2,4-hexadiyne], (PDA-DCHD), where  $\alpha_{\text{exc}} \approx 8200 \text{ \AA}^3$  was obtained from the quadratic Stark shift of the excitons near 2 eV. Therefore, the corresponding exciton binding energy in PPV must be proportionately smaller than that in PDA-DCHD.<sup>39</sup> The polarizability  $\alpha_n$  of a state  $|n\rangle$  is given by the sum over all virtual transitions to all states  $|k\rangle$ ,<sup>39</sup>

$$\alpha_n = \frac{2|\mu_{nk}|^2}{\hbar\omega_{nk}}, \quad (4)$$

where  $\hbar\omega_{nk}$  is the energy gap between  $|n\rangle$  and  $|k\rangle$  (in this case,  $\hbar\omega_{nk} = E_{\text{exc}}$ , the exciton binding energy) and  $\mu_{nk}$  the transition dipole moment. Since the oscillator strength of the intense  $\pi$ - $\pi^*$  transition in PDA-DCHD is comparable to that in PPV and since the exciton binding energy is known to be about 0.4 eV for the polarizability of  $8200 \text{ \AA}^3$  in PDA-DCHD,<sup>39</sup> the enormous value of  $\alpha_{\text{exc}}$

inferred from Eq. (3) sets an upper limit on the exciton binding energy in PPV of less than about 4 meV. Such a small binding energy implies that the initial assumption of a bound exciton is invalid; a binding energy of less than 4 meV is nearly an order of magnitude less than  $k_B T$  at room temperature.

The conclusions are clear.

(i) By assuming that the fast initial photocurrent is a displacement current arising from the polarization of bound excitons, we are able to set an upper limit on the exciton binding energy of less than 4 meV.

(ii) Because this upper limit on the exciton binding energy is nearly an order of magnitude less than  $k_B T$  at room temperature, the fast initial photocurrent is definitively identified as arising from the motion of free charge carriers in the applied electric field.

To verify and confirm these conclusions, we have carried out fast transient photoconductivity experiments on single crystals of polydiacetylene-(toluene sulfonate) (PDA-TS), a system where the intense absorption near 2 eV is to be excitonic with a binding energy of approximately 0.4 eV (established, for example, through the energy difference between the absorption peak and the onset of photoconductivity).<sup>40,41</sup> When pumping directly into the exciton peak, we find that the displacement current [Eq. (3)] is below the level of detectability, i.e., two orders of magnitude below the photocurrent that we observe when pumping into the single particle continuum above 2.4 eV. The small displacement current is consistent with the value expected from Eq. (3) with  $\alpha_{\text{exc}} < 10^4 \text{ \AA}^3$ , as measured independently in the polydiacetylenes.<sup>39</sup>

There are several other aspects of the photoconductivity data which indicate that the fast transient PC is not the displacement current from the field-induced polarization of bound excitons.

(1) In contrast to the stripline response time  $2Z_0C_g \approx 2$  ps,<sup>38</sup> the initial transient PC observed in PPV extends to times  $\geq 100$  ps, i.e., beyond the temporal resolution time of the detection system (50 ps) and therefore inconsistent with the displacement current contribution.

(2) The transient PC in a PPV derivative, poly[2-methoxy, 5-(2'-ethyl-hexyloxy)-*p*-phenylenevinylene] (MEH-PPV), is observed to be at least two orders of magnitude smaller than that in PPV, although the absorption coefficients are similar (and the photoluminescence efficiency is significantly larger in MEH-PPV), inconsistent with a displacement current contribution.<sup>42</sup>

(3) The magnitude and the decay time of the transient PC in MEH-PPV are significantly enhanced when sensitized by as little as 1%  $C_{60}$  even though MEH-PPV dominates the optical absorption. In this case,  $C_{60}$  acts as an electron acceptor to the photoexcited state of MEH-PPV, leading to ultrafast electron transfer,<sup>43-45</sup> which thereby minimizes early time recombination and enhances the quantum yield for free carrier photogeneration.<sup>42</sup>

Since we conclude that the fast transient PC results from the transport of photoexcited charge carriers (rather than from the displacement current due to the polarization of bound neutral excitons), the observed temperature independence of the transient PC is in sharp con-



tradition to the predictions of the Onsager model (see the more extended discussion of this point in the following subsection).<sup>37</sup> The temperature-independent prompt PC can be readily understood, however, as resulting from direct photogeneration of free carriers in the  $\pi$  and  $\pi^*$  bands with subsequent charge carrier transport prior to initial trapping.

#### B. Photogeneration of free charge carriers via the interband ( $\pi$ - $\pi^*$ ) transition

The magnitude of the peak transient photoconductivity in PPV is quite large, comparable to that of *trans*-(CH)<sub>x</sub>;<sup>17</sup> recent measurements of the picosecond PC in *trans*-(CH)<sub>x</sub> (with improved time resolution using a cross-correlation method<sup>22</sup>) yield  $\mu > 20 \text{ cm}^2/\text{Vs}$  for the initial mobility. Thus the relatively large initial photoconductivity implies the fast photogeneration of *mobile* charge carriers.

The combination of soliton-pair confinement and Coulomb attraction after *intrachain* photogeneration of an electron and a hole in nondegenerate ground-state conjugated polymers is expected to lead to rapid formation of neutral polaron excitons.<sup>8</sup> The latter should decay to the ground state by luminescence emission in parallel with rapid nonradiative recombination. The fast decay of the photoinduced bleaching of the interband transition has been interpreted as resulting from the formation and (radiative and nonradiative) decay of the neutral intrachain polaron excitons (or bipolaron excitons).<sup>23,46-48</sup> It was suggested that interchain coupling enables an electron and a hole to be created on different chains, thereby enabling the separation of charged carriers prior to lattice relaxation.<sup>16</sup>

Transient PA measurements showed that self-localization of the photogenerated free carriers occurs within 300 fs,<sup>49</sup> consistent with the prediction of the Su-Schrieffer-Heeger (SSH) model.<sup>1,27</sup> Photoinduced absorption measurements at microsecond times and longer and spin-dependent PA (which measures changes in PA due to resonant absorption of microwaves as a function of magnetic field) indicate that a significant fraction of long-lived photoexcited species are polarons.<sup>49,50</sup>

Because the temperature-dependent slower component of the transient photocurrent shows the square-root intensity dependence (in contrast to the temperature independent initial component which shows a linear intensity dependence), we associate the slower component with bipolarons formed through the coalescence of like-charged polarons which dominate the relatively large, initial picosecond photoconductive response  $P^\pm + P^\pm \rightarrow B^{2\pm}$ . The assignment of the slower component to bipolarons is consistent with the square-root dependence on the excitation pump intensity observed for the photoinduced bipolaron absorption peaks.<sup>10,51</sup> It is well known that in conducting polymers, bipolarons can be lower in energy than separated polarons.<sup>1</sup> From the steady-state PC (Ref. 26) and PA (Refs. 10 and 11) measurements in PPV, the long-lived charge carriers have been identified as bipolarons. The observation of the infrared active vibrational modes and the characteristic

pair of subgap electronic absorption bands indicated the photogeneration of bipolarons.<sup>25</sup> Spin-dependent photomodulation experiments showed that the long-lived charged excitations are associated with spinless features in PA whose recombination (or generation) is spin dependent, consistent with the model of bipolaron generation through the coalescence of like-charged polarons.<sup>13</sup>

The rapid initial decay time is similar to that found in *trans*-(CH)<sub>x</sub> (Refs. 17, 21, and 22) and P3HT (Ref. 20) and in amorphous semiconductors,<sup>52</sup> and probably results from the presence of a relatively high density of deep traps with energies such that the activated probability of release is small even at room temperature. The temperature independence of the (pretrapping) transient photocurrent signal suggests that photoexcitation results in the initial photogeneration of "hot" carriers in extended band states with high mobility, as in *trans*-(CH)<sub>x</sub>.<sup>17,21,22</sup> As the initial carriers (electrons in the conduction band and holes in the valence band) thermalize and recombine, a significant fraction fall into traps that govern the transport at times beyond about 100 ps. Although the probability of activated release from traps is small, it dominates the activated photocurrent from the nanosecond-time regime to the steady state. The observed activation energies of about 100 meV for the slower component of the transient photocurrent and of about 140 meV for the steady-state photocurrent are consistent with the trap-controlled transport in which carriers become progressively more deeply trapped at longer times.

The observation of the temperature-independent, relatively large initial photoconductivity which is proportional to the light intensity and electric field provides crucial information relevant to establishing the mechanism for photogeneration of charged carriers. Gailberger and Bässler<sup>14</sup> and Frankevich *et al.*<sup>15</sup> proposed that, in PPV and its derivatives, charge carriers are photogenerated by electric-field-induced or thermally induced dissociation of excitons in the context of the Onsager model.<sup>37</sup>

Using limited time-resolution (up to several tens of nanoseconds) time-of-flight (TOF) photoconductivity measurements, a thermal activation energy of about 165 meV was inferred and interpreted as the exciton binding energy<sup>14</sup> (note, however, the importance of contact effects in TOF measurements<sup>53</sup>). We show in Figs. 1 and 2, however, that the activated temperature behavior is due to the *slower component* which is responsible for the photoconductivity beyond the nanosecond time scale. The initial fast component in the picosecond time regime is temperature independent, *unambiguously inconsistent with the Onsager model*. We have also observed that the transient peak PC and steady-state PC are linearly proportional to the electric field, again inconsistent with the Onsager model. Moreover, the observed linearity of the initial photocurrent on the light intensity implies direct photogeneration of free carriers (when exciton photogeneration is involved in photoconduction, as in aromatic hydrocarbons,<sup>54</sup> a quadratic intensity dependence is observed in the transient pulsed photoconductivity). These observations indicate that the photogeneration of charge carriers via an interband transition is the primary process; the carriers do not result from thermal dissociation

of excitons. This conclusion is substantiated by the spectral response of the photocurrent: the threshold of both transient and steady-state PC coincides with that of optical absorption at 2.35 eV.

### C. Excitons or free carriers as the primary photoexcitations in PPV: Independent evidence

In Sec. IV A, we demonstrate that the initial fast transient PC arises from motion of separated charge carriers; it is not the displacement current which would arise from the field-induced polarization of bound neutral excitons. In Sec. IV B, we demonstrated that all aspects of the data are consistent with the direct photogeneration of free charge carriers via the interband ( $\pi$ - $\pi^*$ ) transition. In the following paragraphs, we briefly summarize independent evidence that a band model contains the essential physics of the electronic structure of PPV.

The fundamental definition of the single-particle energy gap in a semiconductor is the difference between the energy for electron injection ( $E_{\pi^*}$ ) and the energy for hole injection ( $E_{\pi}$ ), i.e., the difference between chemical reduction and chemical oxidation. In a band model, this energy difference  $E_{\pi^*} - E_{\pi} = E_g$  is the energy gap and it is precisely equal to the energy gap as measured in the interband ( $\pi$ - $\pi^*$ ) optical transition. If, however, the photoexcited electron and hole are bound with an exciton binding energy  $E_{exc}$ , then the optical gap ( $E_{opt}$ ) would be significantly less than the single-particle energy gap:

$$E_{opt} = E_g - E_{exc} . \quad (5)$$

The single-particle energy gap can be determined directly by using electrochemical methods for measuring the voltage difference  $V_{eh}$  between electron injection (reduction) and hole injection (oxidation)  $E_g = eV_{eh}$ , while using the polymer as one electrode in an electrochemical cell. The appropriate electrochemical measurements have been carried out by Eckhardt *et al.*<sup>55</sup> for poly(*p*-phenylene vinylene), poly(thienylene vinylene), and their alkoxy-substituted derivatives. They found that the electrochemically derived band gaps agree well with  $E_{opt}$ , indicating that in all cases  $E_{exc}$  is within the measurement error ( $E_{exc} < 0.1$  eV). Similar agreement between  $E_{opt}$  and  $eV_{eh}$  was obtained earlier for polyacetylene.<sup>56</sup>

In Sec. IV A, we noted that the magnitude and the decay time of the transient PC in MEH-PPV are significantly enhanced when sensitized by as little as 1% C<sub>60</sub> even though MEH-PPV dominates the optical absorption.<sup>42</sup> In these MEH-PPV/C<sub>60</sub> mixtures, the optical absorption is a linear superposition of the absorption from the conducting polymer and the absorption for C<sub>60</sub> with no indication of the formation of a charge transfer complex. C<sub>60</sub> acts as an electron acceptor to the photoexcited state of MEH-PPV, leading to ultrafast electron transfer,<sup>43-45</sup> which thereby minimizes early time recombination and enhances the quantum yield for free carrier photogeneration.<sup>42</sup> If  $E_{exc}$  were significant in MEH-PPV, energy would be required to separate the electron and the hole. Consequently, unless there were evidence of the formation of a charge-transfer complex, the enhanced

transient PC response would be activated with an activation energy comparable to  $E_{exc}$ . Such activated behavior is not observed; the ultrafast photoinduced electron transfer and the resulting enhanced PC response occur at room temperature and below.<sup>42</sup> On the contrary, these ultrafast photoinduced electron-transfer results can be readily understood within a band model of the electronic structure of the PPV derivative.<sup>42-45</sup>

In the exciton model, the strong optical absorption results from a transition from the ground state to a singlet exciton final state. Even if the latter has dispersion due to translational symmetry in an ordered lattice, the transition is "vertical," from the ground state to the  $k=0$  exciton state. As a result, the exciton absorption lineshape in ordered, chain extended and chain aligned material would be symmetric. The symmetric line shape is, in fact, observed as expected in single crystal studies of the polydiacetylenes (where  $E_{exc} \approx 0.4$  eV).<sup>40</sup> The symmetric line shape is not found for PPV and its derivatives. In experiments on gel-processed MEH-PPV blends in polyethylene, the material with the highest-order parameter (as inferred from visible and infrared dichroism and from polarized emission) exhibits an asymmetric line shape.<sup>7</sup> This line shape can be accurately fit by the square-root singularity (broadened by only 0.04 eV due to a combination of interchain coupling and residual disorder) expected for the joint density of states which uniquely characterizes the interband transition in a one-dimensional system.<sup>7</sup> Although the absorption line shape can be fit within the exciton model by assuming a specific distribution of conjugation lengths (characteristic of the disorder in that sample),<sup>57</sup> conservation of oscillator strength would require a large fraction of short segments, inconsistent with the observed emission spectra.<sup>58</sup>

Site-selective fluorescence (SSF) measurements have been interpreted as evidence for bound exciton formation (although the interpretation does not provide an estimate of the exciton binding energy).<sup>57</sup> A more careful analysis, including the requirement of conservation of total oscillator strength, has shown, however, that the results are not consistent with exciton thermalization in a disordered system. Hot carrier thermalization in relatively long conjugated segments is consistent with the SSF data and also consistent with the need to conserve total oscillator strength.<sup>58</sup>

Electroabsorption measurements have been interpreted in terms of the Stark shift of exciton (i.e., an electroabsorption spectrum which closely follows the first derivative of the absorption).<sup>59</sup> We note, however, that the first derivative lineshape can be inferred directly from perturbation theory, *independent of the model* (for example, the exciton model or the band model).<sup>60</sup> In addition, the electroabsorption line shape in MEH-PPV can be accurately fit using the SSH model.<sup>60</sup>

The photoconductivity data and the evidence summarized briefly in this section indicate that the primary singlet photoexcitations are free carriers. Nevertheless, triplet excited states have been observed in photoinduced absorption studies.<sup>11-13</sup> Although the relatively rapid intersystem crossing into the triplet manifold<sup>61</sup> and the efficient quenching of the intersystem crossing<sup>44</sup> by the

even more rapid photoinduced charge transfer<sup>45</sup> imply weak binding, the energy of the lowest triplet state with respect to the single-particle continuum (i.e., the triplet binding energy) has not been determined.

## V. CONCLUSIONS

Transient photoconductivity studies of PPV reveal a fast initial response ( $< 100$  ps), followed by a slower component with a decay time of about 600 ps. The agreement of the onset of both transient and steady-state PC with that of optical absorption in PPV, in conjunction with a relatively large, temperature-independent initial fast transient photoconductivity, implies the photogeneration of free carriers via an interband transition. The magnitude of the fast component is proportional to the light intensity and independent of temperature. The data rule out the direct photogeneration of excitons as the primary excitations in PPV.

The magnitude of the slower component is proportional to the square root of the light intensity and decreases as temperature decreases with a thermal activation energy of about 100 meV. Since charged bipolarons must be formed indirectly via  $P^{\pm} + P^{\pm} \rightarrow B^{2\pm}$ , we attribute the initial temperature-independent response to photogenerated polarons and the following slower decay to bipolarons.

The interpretation of the initial temperature-independent transient photocurrent as the displacement current from the field-induced polarization is ruled out by careful analysis of the transient photocurrent data and by direct measurements on PDA-TS, a conjugated polymer with a known exciton binding energy ( $E_{\text{exc}} \approx 0.4$  eV). A variety of measurements have enabled us to set an upper limit on the exciton binding energy in PPV and several of its alkoxy derivatives;  $E_{\text{exc}}$  is comparable to, or less than,  $k_B T$  at room temperature. Moreover, we have shown that using the band model, the steady-state PC action spectrum can be quantitatively predicted from the experimentally determined absorption spectrum.<sup>26</sup> We conclude, therefore, that the electron-electron interaction is well screened in PPV and that free carriers are directly generated upon photoexcitation of PPV and its derivatives.

## ACKNOWLEDGMENTS

We thank Dr. C. Zhang and Professor F. Wudl for preparation of the PPV. Important discussions with Dr. N. S. Sariciftci and Dr. K. Pakbaz are sincerely appreciated. This work was supported by the National Science Foundation under Grant No. NSF-DMR90-12808.

- <sup>1</sup>A. J. Heeger, S. Kivelson, J. R. Schrieffer, and W.-P. Su, *Rev. Mod. Phys.* **60**, 781 (1988), and references therein.
- <sup>2</sup>J. H. Burroughes, D. D. C. Bradley, A. R. Brown, R. N. Marks, K. Mackay, R. H. Friend, P. L. Burns, and A. B. Holmes, *Nature* **347**, 539 (1990).
- <sup>3</sup>D. Braun and A. J. Heeger, *Appl. Phys. Lett.* **58**, 1982 (1991); D. Braun, G. Gustafsson, D. McBranch, and A. J. Heeger, *J. Appl. Phys.* **72**, 564 (1992).
- <sup>4</sup>G. Gustafsson, Y. Cao, G. M. Treacy, F. Klavetter, N. Colaneri, and A. J. Heeger, *Nature* **357**, 477 (1992).
- <sup>5</sup>P. L. Burns, A. B. Holmes, A. Kraft, D. D. C. Bradley, A. R. Brown, R. H. Friend, and R. W. Gymer, *Nature* **356**, 47 (1992); P. L. Burns, A. B. Holmes, A. Kraft, D. D. C. Bradley, A. R. Brown, and R. H. Friend, *J. Chem. Soc. Chem. Commun.* **32** (1992).
- <sup>6</sup>(a) T. W. Hagler and A. J. Heeger, *Chem. Phys. Lett.* **189**, 333 (1992); (b) *Phys. Rev. B* (to be published).
- <sup>7</sup>T. W. Hagler, K. Pakbaz, K. F. Voss, and A. J. Heeger, *Phys. Rev. B* **44**, 8652 (1991).
- <sup>8</sup>K. Fesser, A. R. Bishop, and D. K. Campbell, *Phys. Rev. B* **27**, 4804 (1983).
- <sup>9</sup>M. Furukawa, K. Mizuno, A. Matsui, S. D. D. V. Rughooputh, and W. C. Walker, *J. Phys. Soc. Jpn.* **58**, 2976 (1989).
- <sup>10</sup>R. H. Friend, D. D. C. Bradley, and P. D. Townsend, *J. Phys. D* **20**, 1367 (1987), and references therein.
- <sup>11</sup>N. F. Colaneri, D. D. C. Bradley, R. H. Friend, P. L. Burn, A. B. Holmes, and C. W. Spangler, *Phys. Rev. B* **42**, 11670 (1990).
- <sup>12</sup>L. Smilowitz and A. J. Heeger, *Synth. Met.* **48**, 193 (1992).
- <sup>13</sup>X. Wei, B. C. Hess, Z. V. Vardeny, and F. Wudl, *Phys. Rev. Lett.* **68**, 666 (1992).
- <sup>14</sup>M. Gailberger and H. Bässler, *Phys. Rev. B* **44**, 8643 (1991).
- <sup>15</sup>E. L. Frankevich, A. A. Lymarev, I. Sokolik, F. E. Karasz, S. Blumstengel, R. H. Baughman, and H. H. Hörhold, *Phys. Rev. B* **46**, 9320 (1992).
- <sup>16</sup>D. D. C. Bradley, Y. Q. Shen, H. Bleier, and S. Roth, *J. Phys. C* **21**, L515 (1988).
- <sup>17</sup>M. Sinclair, D. Moses, and A. J. Heeger, *Solid State Commun.* **59**, 343 (1986).
- <sup>18</sup>D. Moses, M. Sinclair, and A. J. Heeger, *Phys. Rev. Lett.* **58**, 2710 (1987).
- <sup>19</sup>S. D. Phillips and A. J. Heeger, *Phys. Rev. B* **38**, 6211 (1988).
- <sup>20</sup>G. Yu, S. D. Phillips, H. Tomozawa, and A. J. Heeger, *Phys. Rev. B* **42**, 3004 (1990).
- <sup>21</sup>H. Bleier, S. Roth, Y. Q. Shen, D. Schafer-Siebert, and G. Leising, *Phys. Rev. B* **38**, 3004 (1988).
- <sup>22</sup>J. Reichenbach, M. Kaiser, J. Anders, H. Byrne, and S. Roth, *Synth. Met.* **51**, 245 (1992).
- <sup>23</sup>M. B. Sinclair, D. McBranch, T. W. Hagler, and A. J. Heeger, *Synth. Met.* **49-50**, 593 (1992).
- <sup>24</sup>(a) K. S. Wong, D. D. C. Bradley, W. Hayes, J. F. Ryan, R. H. Friend, H. Lindenberger, and S. Roth, *J. Phys. C* **20**, L187 (1987); (b) L. Smilowitz, N. S. Sariciftci, A. J. Heeger, G. Wang, and J. E. Bowers, *J. Chem. Phys.* **98**, 6504 (1993).
- <sup>25</sup>K. F. Voss, C. M. Foster, L. Smilowitz, D. Mihailovic, S. Askari, G. Srdanov, Z. Ni, S. Shi, A. J. Heeger, and F. Wudl, *Phys. Rev. B* **43**, 5109 (1991).
- <sup>26</sup>C. H. Lee, G. Yu, and A. J. Heeger, *Phys. Rev. B* **47**, 15543 (1993).
- <sup>27</sup>W. P. Su and J. R. Schrieffer, *Proc. Natl. Acad. Sci. (U.S.A.)* **77**, 5626 (1980).
- <sup>28</sup>A. O. Patil, S. D. D. V. Rughooputh, and F. Wudl, *Synth. Met.* **29**, E115 (1989).
- <sup>29</sup>D. H. Auston, in *Picosecond Optoelectric Devices*, edited by C. H. Lee (Academic, New York, 1984), Chap. 4.
- <sup>30</sup>H. Li, S. Rentsch, J. Yang, M. Lenzner, and H. Bergner, *Phys. Status Solidi B* **162**, 545 (1990).
- <sup>31</sup>Y. Yacoby, S. Roth, K. Menke, F. Keilmann, and J. Kuhl, *Solid State Commun.* **47**, 869 (1983).

- <sup>32</sup>N. F. Mott and E. A. Davis, *Electronic Processes in Non-Crystalline Materials* (Clarendon, Oxford, 1979).
- <sup>33</sup>A. J. Epstein, in *Handbook of Conducting Polymers*, edited by T. A. Skotheim (Dekker, New York, 1986), Vol. 2, p. 1041.
- <sup>34</sup>S. Tokito, T. Tsutsui, R. Tanaka, and S. Saito, *Jpn. J. Appl. Phys.* **25**, L680 (1986).
- <sup>35</sup>S. D. Phillips, G. Yu, Y. Cao, and A. J. Heeger, *Phys. Rev. B* **39**, 10702 (1989).
- <sup>36</sup>H. B. DeVore, *Phys. Rev.* **102**, 86 (1956).
- <sup>37</sup>L. Onsager, *Phys. Rev.* **54**, 554 (1938).
- <sup>38</sup>M. Maeda, *IEEE Trans. Microwave Theory Tech.* **MTT-20**, 370 (1972).
- <sup>39</sup>G. Weiser, *Phys. Rev. B* **45**, 14076 (1992).
- <sup>40</sup>R. R. Chance and R. H. Baughman, *J. Chem. Phys.* **64**, 3889 (1976).
- <sup>41</sup>K. Lochner, H. Bäessler, B. Tieke, and G. Wegner, *Phys. Status Solidi B* **88**, 653 (1978); A. S. Siddiqui, *J. Phys. C* **13**, 2147 (1980).
- <sup>42</sup>C. H. Lee, G. Yu, D. Moses, K. Pakbaz, C. Zhang, N. S. Sariciftci, A. J. Heeger, and F. Wudl, *Phys. Rev. B* **48**, 15425 (1993).
- <sup>43</sup>N. S. Sariciftci, L. Smilowitz, A. J. Heeger, and F. Wudl, *Science* **258**, 1474 (1992).
- <sup>44</sup>L. Smilowitz, N. S. Sariciftci, R. Wu, C. Gettinger, A. J. Heeger, and F. Wudl, *Phys. Rev. B* **47**, 13835 (1993).
- <sup>45</sup>B. Kraabel, C. H. Lee, D. McBranch, D. Moses, N. S. Sariciftci, and A. J. Heeger, *Chem. Phys. Lett.* **213**, 389 (1993).
- <sup>46</sup>T. Kobayashi, M. Yoshizawa, U. Stamm, M. Taiji, and M. Hasegawa, *J. Opt. Soc. Am. B* **7**, 1558 (1990).
- <sup>47</sup>I. D. W. Samuel, K. E. Meyer, D. D. C. Bradley, R. H. Friend, H. Murata, T. Tsutsui, and S. Saito, *Synth. Met.* **41-43**, 1377 (1991).
- <sup>48</sup>S. D. Halle, M. Yoshizawa, H. Murata, T. Tsutsui, S. Saito, and T. Kobayashi, *Synth. Met.* **49-50**, 429 (1992).
- <sup>49</sup>G. S. Kanner, X. Wei, B. C. Hess, L. R. Chen, and Z. V. Vardeny, *Phys. Rev. Lett.* **69**, 538 (1992).
- <sup>50</sup>G. S. Kanner and Z. V. Vardeny, *Synth. Met.* **49-50**, 611 (1992).
- <sup>51</sup>A. J. Brasnet, N. F. Colaneri, D. D. C. Bradley, R. A. Lawrence, R. H. Friend, H. Murata, S. Tokito, T. Tsutsui, and S. Saito, *Phys. Rev. B* **41**, 10586 (1990).
- <sup>52</sup>A. M. Johnson, D. H. Auston, P. R. Smith, J. C. Bean, J. P. Harbison, and A. C. Adams, *Phys. Rev. B* **23**, 6816 (1981).
- <sup>53</sup>In previous studies of transient photoconductivity of PPV (see Ref. 14), thermally activated transport and a superlinear dependence of the photocurrent on external field were found, observations that have invoked the Onsager theory of carrier generation (Ref. 37). However, since these previous measurements used steady-state photoconductivity and TOF measurements, they were limited in two respects. (a) The temporal resolution was not adequate for resolving the initial temperature independent contribution that precedes the slower thermally activated contribution. (b) The results were dominated by the built-in potential barrier at the semiconductor-metal contact. Comparative studies of the transient photoconductivity of *a*-Se measured by Auston stripline switch technique and by the TOF technique [see D. Moses, *Philos. Mag.* **66**, 1 (1991)] demonstrate that the results are dependent on the sample measuring configuration. In the TOF measurements, the sample is illuminated through a semitransparent metallic electrode, near the depletion region at the semiconductor-metal junction. Therefore, in this case, *all* the excited carriers confront a potential barrier, and the carrier generation (e.g., thermionic emission from the metal contact) is indeed thermally activated and exponentially dependent on external bias, as in photodiode. By comparison, in transient photoconductivity measurements which utilize the Auston stripline switch technique, the polymer surface within the gap between electrodes is directly illuminated. Thus the majority of the carriers are photogenerated far from the contacts. For the magnitude of currents used in our studies, the contact effects have been found to be negligible. Thus the reasons for the disparity between the previous results (Ref. 14) and those presented in this report can be understood. It appears that while the TOF measurements are useful for measuring the carrier mobility operative during the trap-limited transport, the TOF technique is not adequate for investigating the intrinsic properties of the prompt photoconductivity. In addition to the problems associated with the potential barrier at the PPV-metal contact, the data showing thermally activated transient photoconductivity and its strong (superlinear) dependence on external field (Ref. 14) were dominated at the longer times involved in the TOF measurement by transport of thermalized carriers associated with the slow photoconductive component rather than the prompt initial contribution.
- <sup>54</sup>G. Castro, *IBM J. Res. Dev.* **15**, 27 (1971).
- <sup>55</sup>H. Eckhart, L. W. Shacklette, K. Y. Jen, and R. L. Elsenbaumer, *J. Chem. Phys.* **91**, 1303 (1989).
- <sup>56</sup>J. H. Kaufman, J. W. Kaufer, A. J. Heeger, R. Kaner, and A. G. MacDiarmid, *Phys. Rev. B* **26**, 2327 (1982).
- <sup>57</sup>U. Rauscher, H. Bäessler, D. D. C. Bradley, and M. Hennecke, *Phys. Rev. B* **42**, 9830 (1990).
- <sup>58</sup>T. Hagler, K. Pakbaz, and D. McBranch (unpublished).
- <sup>59</sup>C. Botta, G. Zhuo, O. M. Gelsen, D. D. C. Bradley, and A. Musco, *Synth. Met.* **55-57**, 85 (1993).
- <sup>60</sup>T. W. Hagler, K. Pakbaz, and A. J. Heeger (unpublished).
- <sup>61</sup>M. B. Sinclair, D. McBranch, T. W. Hagler, and A. J. Heeger, *Synth. Met.* **49-50**, 593 (1992).